Laser chirp controlled relativistic few-cycle mid-infrared pulse generation: Supplementary information

Dongao Li[1], Guobo Zhang[2], Jie Zhao[1], Yanting Hu[1], Yu Lu[1], Hao Zhang[1], Qianni Li[1], Dongze Zhang[1], Rong Sha[1], Fuqiu Shao[1], Zhengming Sheng[3,4,5], and Tongpu Yu[1]

[1]Department of Physics, National University of Defense Technology, Changsha 410073, China.
[2]Department of Nuclear Science and Technology, National University of Defense Technology, Changsha 410073, China.
[3]Key Laboratory for Laser Plasmas (MOE) and School of Physics and Astronomy, Shanghai Jiao Tong University, Shanghai 200240, China.
[4]Collaborative Innovation Center of IFSA, Shanghai Jiao Tong University, Shanghai 200240, China.
[5]Tsung-Dao Lee Institute, Shanghai Jiao Tong University, Shanghai, 201210, China.

Abstract
The supplement is organized as follows: in Section 1, the robustness in our scheme is investigated. In Section 2, we show the effect of PCLP on the Mid-IR generation for comparison. Finally, the 3D simulations with NCLP and un-chirp pulses are discussed in Section 3.

Keywords: mid-infrared generation; photon deceleration; chirp laser pulses; laser wakefield

1. Robustness of the scheme

To study the robustness of the scheme, we show the effect of on-axis plasma density and down ramp length on the energy conversion efficiency of the Mid-IR pulse by using the two-dimensional (2D) simulation. Table S1 shows the energy conversion efficiency of the generated Mid-IR pulse with different on-axis plasma density, the initial laser intensity and the plasma configuration are consistent with in Figure 1. When the on-axis plasma density is 3×10^{18} cm^{-3}, the energy conversion efficiency of 5.0% at $t = 4125\mathrm{T}_0$ is the maximum energy conversion efficiency. However, when the on-axis plasma density drops to 2.5×10^{18} cm^{-3}, the energy conversion efficiency of the generated Mid-IR pulse approaches 2.6%. This is because that the drive laser pulse does not completely turn to Mid-IR pulse at $t = 4125\mathrm{T}_0$. In the higher density plasma, the Mid-IR pulse can be generated quickly. In the case of 3.5×10^{18} cm^{-3}, the length of 3300 μm of plasma exceeds the best length of generation Mid-IR pulses. After the best position, the energy conversion efficiency of long wavelength Mid-IR pulse is decreased greatly. Due to the bubble is full of Mid-IR pulses, the Mid-IR pulse will experience the photon acceleration at the bubble tail. The photon acceleration can make the part of Mid-IR pulses decrease, which reduce the energy and the energy conversion efficiency of long wavelength Mid-IR pulse.

Table S1. The energy conversion efficiency of generated Mid-IR pulses with different plasma density at $t = 4125\mathrm{T}_0$.

n_0 (cm^{-3})	Efficiency	Width (μm)
2.5×10^{18}	2.6%	6.2–26.7
3×10^{18}	5.0%	4.2–20.0
3.5×10^{18}	2.1%	5.7–26.7

The down ramp at the end of plasma can guide pulses to leave the plasma. Table S2 provides the energy conversion efficiency of the generated Mid-IR pulse with different down ramp length. All simulations of different down ramp length have the same length and density of plateau, which is the main area of pulses compression and conversion. It can be seen in Table S2, the energy conversion efficiency is decreased when the down ramp is increased.

Correspondence to: G. Zhang. Department of Nuclear Science and Technology, National University of Defense Technology, Changsha 410073, China. T. Yu. Department of Physics, National University of Defense Technology, Changsha 410073, China. Email: zgb830@163.com (G. Zhang), and tongpu@nudt.edu.cn (T. Yu).

Table S2. The energy conversion efficiency of generated Mid-IR pulses with different down ramp length.

L_f (μm)	Efficiency	Width (μm)
50	5.0%	4.2–20
100	4.8%	4.2–20
200	4.3%	4.2–20
300	3.7%	4.2–20

2. Effect of PCLP on the Mid-IR generation

In order to highlight the advantage of the proposed scheme, we also investigate the effect of positively chirped laser pulses (PCLP), i.e., higher frequency first and lower frequency second, with the chirp parameter $b = 0.07$. Figures S1(a) – S1(c) show the evolution of the PCLP and the plasma density. The parameters of laser and plasma are the same as in the case in Figure 2 of main text. We can see that, the bubble is full of the electromagnetic wave, which is mainly composed of two parts, one is from the nonlinear effect of PCLP, e.g., group velocity dispersion (GVD), and the other is from photon deceleration. Figure S1(d) shows that the spectral distribution of the on-axis laser electric field at $t = 150\mathrm{T}_0$ (blue), $t = 1800\mathrm{T}_0$ (black) and $t = 3600\mathrm{T}_0$ (red), and the inset is the temporal profile of the Mid-IR electric field with the duration of FWHM about 55 fs at $t = 3600\mathrm{T}_0$.

Due to the plasma etching in the wakefield, the rise edge of the PCLP becomes steeper during the pulse propagation, and the increasing pondermotive force enhances the generation rate of the Mid-IR pulse.

For $b = 0.07$, the density perturbation exceeds 1.8×10^{19} cm^{-3} and the refractive index gradient $\partial\eta/\partial\xi \approx -3.8 \times 10^{-3}$ μm^{-1} at $t = 2700\mathrm{T}_0$. For PCLP, one can obtain a Mid-IR of the center wavelength of $\lambda_c = 8.4$ μm, the intensity of $a_{MIR} \approx 1.8$, the number of optical cycles of about 2, and the energy conversion efficiency of only about 1% at $t = 3600\mathrm{T}_0$. This is due to the fact that the PCLP is elongated in the bubble, so that only a part of the drive laser pulse enters the region of negative refractive index gradient to generate the Mid-IR pulse, which can lead to a lower energy conversion efficiency.

3. Evolution and comparison of 3D simulation with NCLP and un-chirp pulse

Figure S2 shows the evolution of the transverse electric field and plasma density. It can be seen that the drive pulse is compressed longitudinally due to the plasma etching and the photon acceleration, which enhances the intensity of the drive laser pulses. Meanwhile, due to the more intense focus of laser pulse in the 3D simulation, a large number of electrons are injected into the bubble. When the NCLP propagates 4 mm in plasma, the Mid-IR pulse slips backwards into the bubble, as shown in Figure S2(f). For the generated Mid-IR pulse at $t = 5000\mathrm{T}_0$, the central wavelength is 6 μm, the intensity is $a_{MIR} \approx 3.5$, and the FWHM duration is 80 fs. Further, the maximum energy conversion efficiency can reach 6.3% at $t = 5300\mathrm{T}_0$.

Figures S3(a)-S3(e) show the evolution of the transverse electric field and plasma density in the case of un-chirp laser pulses for comparison. The parameters of plasma are the same as the case of NCLP. It can be seen that the compression of the drive laser pulse is not obvious in the longitudinal direction. The slow compression of un-chirp laser pulse in the longitudinal direction is a important reason to reduce the energy conversion efficiency of generation Mid-IR pulses. Compared with the NCLP, when the un-chirp laser pulse propagates 4 mm in plasma, we do not observe the Mid-IR pulse in the bubble, as shown in Figure S3(f). Figure S3(g) shows the spectra of on-axis electric field at $t = 50\mathrm{T}_0$ and $t = 5000\mathrm{T}_0$, respectively. It can be seen that the wavelength of laser pulses are around 0.8 – 2 μm, and there are no Mid-IR pulses with wavelength larger than 2 μm in the spectrum.

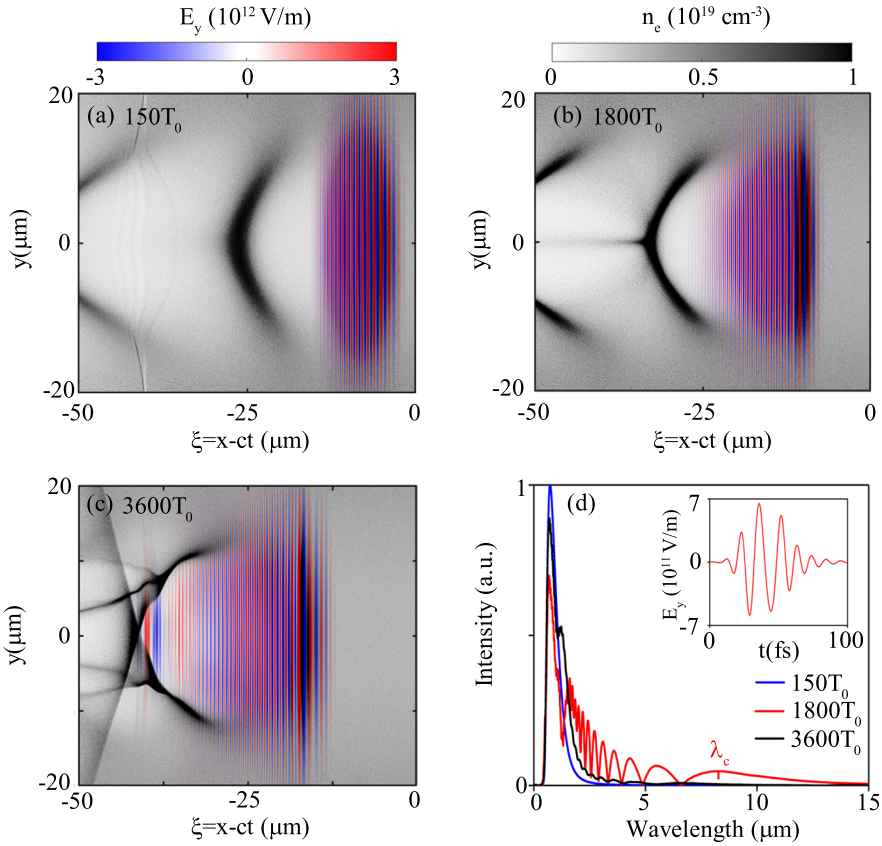

Figure S1. Simulation of laser wakefield excitation and photon deceleration with PCLP. (a)–(c) The distributions of the plasma density (n_e) and the transverse electric field (E_y) at $t = 150\mathrm{T}_0$, $t = 1800\mathrm{T}_0$, and $t = 3600\mathrm{T}_0$. (d) Spectral distribution of the on-axis laser electric field at $t = 150\mathrm{T}_0$ (blue), $t = 1800\mathrm{T}_0$ (black) and $3600\mathrm{T}_0$ (red). The inset is the temporal profile of the Mid-IR electric field at $t = 3600\mathrm{T}_0$.

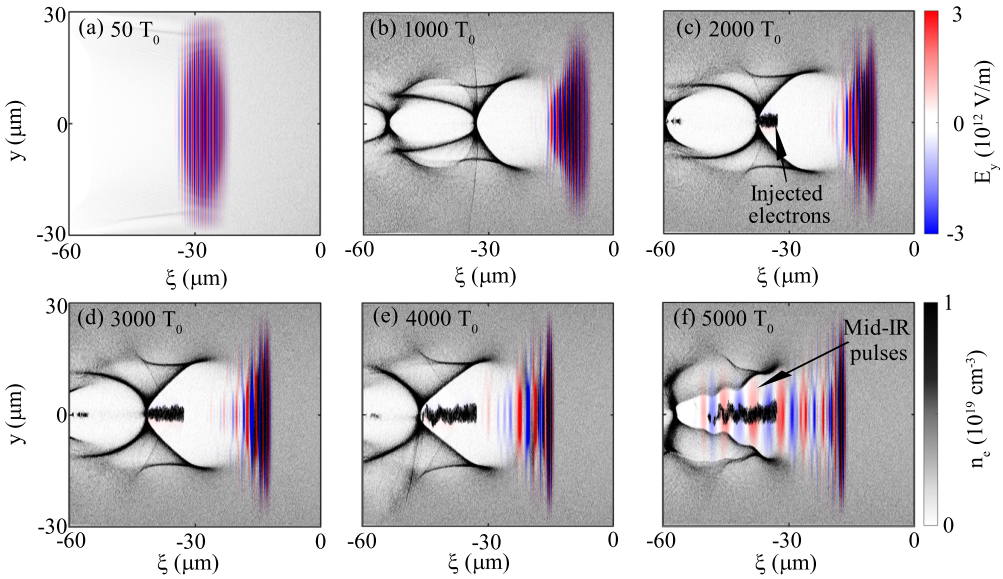

Figure S2. 3D simulation of wakefield excitation and photon deceleration with NCLP. (a)-(f) show snapshots of the distributions of the plasma density (n_e) and the transverse electric field (E_y) at different times.

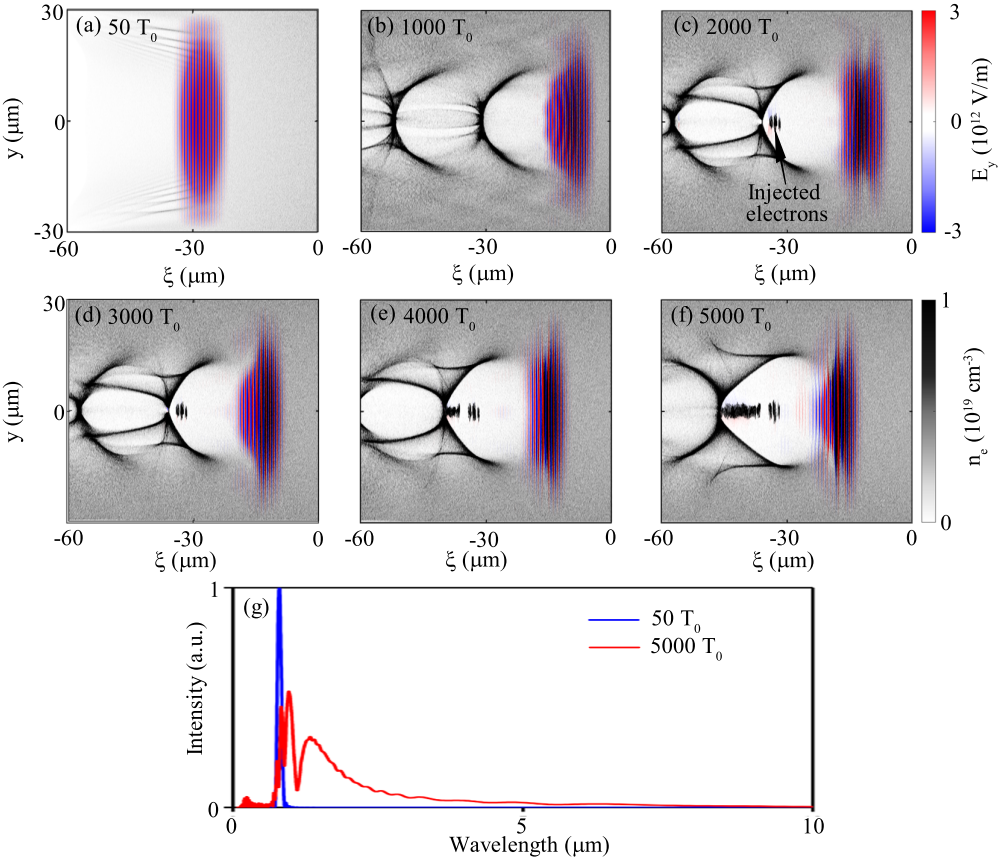

Figure S3. 3D simulation of wakefield excitation and photon deceleration with an un-chirped laser pulse. (a)-(f) show snapshots of the distributions of the plasma density (n_e) and the transverse electric field (E_y) at different times. (g) Spectral distribution of the on-axis laser electric field at $t = 50\mathrm{T}_0$ and $t = 5000\mathrm{T}_0$.